Future Foods 12 (2025) 100725

Contents lists available at ScienceDirect

Future Foods

journal homepage: www.elsevier.com/locate/fufo

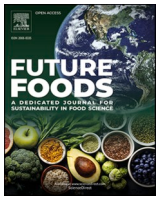

Influence of starch-based gels on 3D food printing: Linking printability, texture, rheological properties, and sensory evaluation

Taíse Toniazzo [a,b], Cassandre Leverrier [b], Nathália Lisboa Souza [b,c], Giana Almeida [b], Carmen Cecília Tadini [a], Valérie Guenard-Lampron [b,*]

[a] Universidade de São Paulo, Escola Politécnica, Dept. of Chemical Eng., Main Campus, SP, Brazil. Universidade de São Paulo, FoRC/NAPAN - Food Research Center
[b] Université Paris-Saclay, INRAE, AgroParisTech, UMR SayFood, 91120, 22 Place de l'Agronomie, Palaiseau, France
[c] São Paulo State University –UNESP, Campus of São José do Rio Preto, R. Cristóvão Colombo, 2265 - Jardim Nazareth, São José do Rio Preto-SP, 15054-000, Brazil

ARTICLE INFO

Keywords:
Extrusion-based printing
Recovery
Sensory descriptors
Shear-thinning behavior
Starch
Stickiness
Texture profile analysis

ABSTRACT

3D printing can create personalized food products with three-dimensional shapes and desirable textures. This study investigated the effect of different starch sources (wheat, maize, tapioca, and waxy), with or without kappa-carrageenan (KC), on the printability and sensory properties of starch-based gels. All starch-based gels showed shear-thinning behavior, but only those produced with wheat or maize starch, with or without KC, were able to form and maintain layers, showing the flow behavior index (n) varying from (0.36 – 0.46). The presence of KC in printable starch-based gels led to a decrease in apparent viscosity. For instance, Maize and Maize+KC presented apparent viscosity values of (6295.35 and 3398.80) Pa s, respectively. All printable starch-based gels exhibited $G' > G''$, and Tan $\delta < 1$, indicating high structuration. Wheat and Wheat+KC presented G' and G'' values of (4422 and 853; 3938 and 869) Pa, respectively. Non-printable starch-based gels exhibited fluid-like behavior, showing no support for 3D food printing. Tapioca and Tapioca+KC presented G' and G'' values of (187 and 182; 302 and 252) Pa, respectively. Sensory evaluation showed that 3D-printed cylinders produced with wheat and maize starch without KC were perceived as more viscous, firm, and adhesive in the mouth compared to those made with KC. Hardness instrumentally measured, which was of (1.02 and 0.65) N for Wheat and Wheat+KC, respectively, was correlated with the firmness perceived in sensory evaluation. As a result, this study enhances the understanding of formulation behavior and can support future strategies for developing 3D-printed foods with desirable textural properties.

1. Introduction

3D food printing is a recent technique for producing customized and personalized food products with three-dimensional shapes. Its use has been growing among consumers due to advances in digital technologies, which enable greater precision and innovation in food development (Hussain et al., 2022; Masbernat et al., 2021). Also known as additive manufacturing, this technique constructs objects layer by layer, based on previously designed digital files (Liu et al., 2019; Rayna and Striukova, 2016). In the food industry, 3D printing offers several advantages, especially the ability to produce complex and individualized structures that are often difficult to achieve using conventional production methods (Cotabarren et al., 2023; Qiu et al., 2023).

For an ingredient to be suitable for 3D food printing, it must flow easily through the printer nozzle and retain its structure and stability after printing (Lille et al., 2018). Among the ingredients used in 3D printing formulations, starch is considered an interesting option due to its wide availability, low cost, and ability to form structured gels. Starch is a polysaccharide in higher plants, mainly composed of amylose and amylopectin. Both polymers are arranged in semicrystalline granules with variable porosity, which are highly hydrophilic. The gelatinization process occurs when starch granules are heated in excess water (Appelqvist and Debet, 1997; BeMiller and Whistler, 2009). Thus, starch has gained attention as a promising material, as it presents the requirements for printability (Bitencourt et al., 2023; Cui et al., 2022; Guedes et al., 2023). However, the molecular structure of starch, specifically the ratio of linear (amylose) to branched (amylopectin) starch, significantly impacts its 3D printing performance. The higher amylose content in starch gels enhances the storage modulus and supports the performance of printed products by promoting the formation of

* Corresponding author at: Université Paris-Saclay, INRAE, AgroParisTech, UMR SayFood, 91120, 22 Place de l'Agronomie, Palaiseau, France.
E-mail address: valerie.guenardlampron@agroparistech.fr (V. Guenard-Lampron).

https://doi.org/10.1016/j.fufo.2025.100725
Received 29 May 2025; Received in revised form 10 July 2025; Accepted 20 July 2025
Available online 26 July 2025

cross-linked gel structures and crystalline structures. It also makes extrusion difficult, leading to intermittent extrusion and rough printed morphology (Cheng et al., 2024b; Ji et al., 2022). Short amylopectin chains reduce the degree of short-range order and hydrogen bonding interactions, which is detrimental to the storage modulus and yield stress, negatively affecting the printing precision (Cheng et al., 2023; Ji et al., 2022). Conversely, the higher content of short amylopectin chains facilitates smooth extrusion during the 3D printing process (Ji et al., 2022).

Carrageenans are water-soluble sulfated polysaccharides extracted from red seaweed (Campo et al., 2009; Lascombes et al., 2017). Ideally, they are composed of a repeating unit of disaccharides consisting mainly of galactose sulfate esters and 3,6-anhydrogalactose polysaccharides. Carrageenans exist in three main forms (kappa, iota, and lambda), where kappa and iota carrageenan can form thermoreversible gels in the presence of gel-promoting cations (Lascombes et al., 2017; Rochas et al., 1980). Thus, KC is considered an additive that can be added to improve the gel properties of starch, achieving better printing performance by changing structural characteristics (Bitencourt et al., 2023; Rong et al., 2023).

The interactions between starch and KC can significantly influence their suitability for 3D printing applications. Mechanisms of interaction between starch and KC have been reported in some studies. Matignon et al. (2014a) showed that carrageenan can adsorb on and penetrate starch granules, affecting the microstructure and rheological properties of the mixture. Lascombes et al. (2017) also demonstrated that this interaction is influenced by the charge density of carrageenan, with lower charge densities promoting stronger interactions. Liu et al. (2021, 2022) showed that the rheological properties of starch-KC mixtures are crucial for their functionality. For instance, the addition of KC can increase the gel strength and modify the viscosity of the mixture, which is essential for 3D printing applications. Liu et al. (2021) also optimized the concentration of KC to 0.75 g/100 g for stable gel formation with starch, providing a homogeneous network and stable structure during storage. Matignon et al. (2014b) showed that the microstructure of starch-KC mixtures can vary depending on the blending order and the presence of other components. For example, in ternary mixtures with milk proteins, the interactions between starch and KC are less pronounced. Therefore, rheological knowledge of formulations is essential to improve printability in 3D food printing (Liu et al., 2019). Rheological parameters such as apparent viscosity, yield stress, and viscoelastic behavior are critical to estimate the performance of formulations during and after 3D extrusion-based printing (Chen et al., 2019; Cheng et al., 2024b; Ji et al., 2022; Kozu et al., 2025; Xie et al., 2009). Furthermore, the performing of a recovery test is relevant to simulate shear during extrusion and to evaluate the ability to recover its structure after the process.

In addition to rheological analyses of formulations, it is essential to consider the sensory evaluation of the 3D-printed structures developed. Studies on 3D-printed foods have focused mainly on the influence of printing parameters and the textural characteristics of food formulations on printability. However, to advance the investigation, the connection between sensory aspects, rheological parameters, and instrumentally measured textural properties of 3D-printed foods remains limited (Mirazimi et al., 2023; Severini et al., 2018). For instance, 3D-printed foods present a layer-by-layer structure with a distinct appearance, which can impact their sensory perception. Additionally, polysaccharides added to the formulation may influence the texture and mouthfeel perceived by consumers (Chow et al., 2021; Severini et al., 2018).

To date, few studies have investigated the combined effects of printability, rheological properties, or texture with the sensory evaluation of 3D-printed food. Thus, this work intends to advance in the field by linking it with sensory evaluation (Chow et al., 2021; Mantihal et al., 2019; Markovinovic et al., 2024; Mirazimi et al., 2023; Ren et al., 2023; Riantiningtyas et al., 2021; Tsai and Lin, 2022). In addition, no studies have been found comparing all these effects in 3D-printed foods formulated mainly with different starch sources.

This study aimed to develop formulations with different texture characteristics, using different starch sources, with or without KC. The effects of rheological behavior on the printability of these formulations were investigated and a link was established between printability, rheological properties, texture, and sensory evaluation of the 3D-printed cylinders.

2. Materials and methods

2.1. Materials

Wheat (C Gel™ 20006), tapioca (C CreamGel 70001), maize (C Gel™ 03401), waxy maize (C Gel™ 04201) native starches, maltodextrin (C Dry™ MD 01958 – enzymatic conversion of waxy maize starch), and Kappa-Carrageenan (Satiagel™ RPM 87 R1) were donated by Cargill (Castelmassa, RO, Italy). The glucose syrup (Vahiné, Avignon, France) was purchased in a local supermarket. The citric acid used to formulate the starch-based gels was obtained from Louis Francois (Croissy Beaubourg, France). Ultrapure water (18.2 MΩ/cm, PURELAB Chorus, ELGA Lab water, Veolia, USA) was used throughout the experiments. All chemicals used for the experimental analyses were of analytical grade. In contrast, the chemicals for the sensory analyses were of food grade.

2.2. Methods

2.2.1. Preparation of starch-based gels by gelatinization process and morphological analysis

Starch-based gels were formulated according to Bitencourt et al. (2023), with some modifications supported by preliminary trials. Maltodextrin, citric acid solutions, and KC dispersion were previously prepared, using ultrapure water (PURELAB Chorus, ELGA Lab water, Veolia, USA) at a concentration of 50 g/100 g, 30 g/100 g, and 3 g/100 g, respectively. The KC dispersion was magnetic stirring for 24 h at room temperature (20°C). The prepared maltodextrin, citric acid solutions, and KC dispersion were used to produce the starch-based gels (also prepared without KC). Firstly, 0.6 g/100 g of KC dispersion, 13 g/100 g of maltodextrin solution, 10 g/100 g of glucose syrup, 0.4 g/100 g of citric acid solution, and 15 g/100 g of defined starch were mixed. Ultrapure water (PURELAB Chorus, ELGA Lab water, Veolia, USA) was then added to complete the mixture to 100 g. A citric acid solution was used in starch-based gel formulations to create a slightly acidic sensory perception. Furthermore, a maltodextrin solution was used, as it could decrease the viscosity of the starch-based gel formulation, assisting the 3D food printing process. Starch-based gels were produced with wheat, maize, tapioca, or waxy maize, with KC (acronyms: Wheat+KC, Maize+KC, Tapioca+KC, and Waxy+KC) or without KC (acronyms: Wheat, Maize, Tapioca, and Waxy). After that, the beaker containing the mixture was accommodated in a container with 900 mL of water at 90°C, under continuous stirring (250 rpm) for 20 min, using a mechanical agitation (IKA® Eurostar 60 Control, IKA-Werke GmbH, Staufen, Germany) and a hot plate (Heidolf, MR Hei-Standard, D-91126, Schwabach, Germany). The temperature was monitored (Heidolph, EKT Hei-Con, Schwabach, Germany) and recorded every minute during the gelatinization process to obtain the mean temperature (T_{mean}) and the final temperature (T_{final}). At the end of the gelatinization process, the starch-based gels were placed in a Foodini 3D printer stainless steel capsule (100 mL) with a 1.5 mm nozzle, and the bottom plunger was pressed to remove the air. The starch-based gels were kept at room temperature (20°C) before analysis and 3D food printing, which were performed on the same day.

The morphology of the starch-based gels before and after the gelatinization process, without and with polarized light, was obtained using an Olympus BX-51 microscope (Olympus Optical Co. Ltd., Tokyo, Japan). Images were acquired using a Basler A102fc digital camera

(Basler AG, Ahrensburg, Germany) under 40 × magnification.

2.2.2. Characterization of starch-based gels

2.2.2.1. Determination of pH of starch-based gels. The pH was measured in a 0.05 mg/100 mL aqueous solution of starch-based gels in ultrapure water (PURELAB Chorus, ELGA Lab water, Veolia, USA), using a pH meter (PHenomenal, VWR®, International Ltd, Lutterworth, England).

2.2.2.2. Rheological properties of starch-based gels. Rheological measurements on starch-based gels were performed using a stress-controlled rheometer (Physica, MCR301, Anton Paar), using a parallel plate geometry PP 25 (24.982 mm diameter, GAP of 1 mm). The linear viscoelastic behavior was determined by sweeping the amplitude over a strain range of 0.1 to 100 % and at a fixed frequency of 1 Hz. After that, the flow curves were obtained by registering shear stress (Pa) when the shear rate was increased from 0.1 – 100 s^{-1}.

The data obtained from flow curves were fitted applying the Herschel-Bulkley model and power-law model (Steffe, 1996), using the Statgraphics Centurion 19 software (StatPoint, USA), according to Eqs. (1) and (2), respectively.

$$\tau = \tau_0 + K\dot{\gamma}^n \quad (1)$$

$$\tau = K\dot{\gamma}^n \quad (2)$$

wherein τ is the shear stress (Pa), τ_0 is the yield stress (Pa), K refers to the consistency coefficient (Pa s^n), $\dot{\gamma}$ is the shear rate (s^{-1}), and n denotes the flow behavior index (-).

The tan delta parameter (Tan δ) was also used to describe the viscoelastic behavior of starch-based gels. This parameter is directly related to the energy lost per cycle divided by the energy stored per cycle (Steffe, 1996) and was calculated according to Eq. (3).

$$\tan(\delta) = \frac{G''}{G'} \quad (3)$$

wherein G' is the shear storage modulus (Pa), and G'' is the shear loss modulus (Pa).

After performing the mentioned rheological analyses, the starch-based gel sample was changed and the recovery test was performed, which occurred in three different steps: (1) G' and G'' were recorded at rest at a constant frequency (1 Hz), and strain (0.1%) for 120 s, (2) then, a constant shear of 300 s^{-1} was applied for 40 s and, finally, (3) the first step was repeated to assess structural recovery. The maximum shear rate of 300 s^{-1} used in the second stage of the recovery test was calculated to simulate the shear during extrusion printing. Flow in a tubular geometry for non-Newtonian fluids was considered, according to Eq. (4) (Steffe, 1996):

$$\dot{\gamma}_{max} = \left(\frac{3n+1}{4n}\right)\frac{4\dot{Q}}{\pi R^3} \quad (4)$$

wherein $\dot{Q}$ is the volumetric flow rate (m^3 s^{-1}), R is the nozzle radius (m), and n is the flow behavior index (-).

The shear recovery capacity of printable starch-based gels was determined as the percentage of G' average obtained in 30 s in the third step after a high shear rate (300 s^{-1}) and the average of initial G' obtained in the first step (Achayuthakan and Suphantharika, 2008; Liu et al., 2019). All rheological analyses were performed at a controlled temperature of 20°C, and the data obtained were in duplicate.

2.2.2.3. Stickiness of starch-based gels. The stickiness of the starch-based gels was measured using a texture analyzer (TA. HD.plus, Stable Micro Systems Ltd, Godalming, Surrey, UK) coupled with a 40 mm diameter compression plate geometry (P/35, Stable Micro Systems Ltd., Godalming, England). The pre-test speed was 0.50 mm s^{-1}, the test speed of 1.00 m s^{-1}, and the post-test speed of 1.00 mm s^{-1}. The applied force above the surface of the starch-based gel was 3 N with a contact time of 30 s. The sample preparation involved placing the starch-based gel surface flat against the cylindrical container (diameter of 45 mm and height of 3 mm). The cylindrical container was fixed to the equipment, and the maximum unload force (N) obtained was considered the stickiness value of the starch-based gels. The tests were carried out at room temperature (20°C) with eight repetitions of each formulation.

2.2.3. 3D food printing of starch-based gels

The starch-based gels were printed at 20 °C on a Foodini 3D food printer (Natural Machines, Spain). The main parameters used in the 3D food printer were: distance between layers of 1.6 mm, first layer speed of 100 %, nozzle diameter of 1.5 mm, and line thickness of 1.4 mm. Contrary to conventional 3D food printers that use direct control over printing parameters (e.g., extrusion pressure and flow rate), the Foodini operates with volume extrusion and adjusts the ingredient flow speed to accommodate various food inks (Leam et al., 2024). Consequently, the printing speed was measured by printing a 90 mm straight line of the printable starch-based gels. The printing speed was acquired by dividing the average length of the printed straight line using the printable starch-based gels by the average time taken for each print, resulting in a printing speed of 28 mm s^{-1}. This printing speed was used to calculate the maximum shear rate in Section (2.2.2.2).

The starch-based gels were printed in a filled cylinder format with a diameter of 2.035 cm and a height of 2.045 cm, corresponding to a volume of 6.65 cm^3, named 3D-printed cylinders. The format was externally created (Blender 4.2 LTS) and imported as STL files in the Foodini system.

The 3D-printed cylinders were directly printed on the Foodini silicone mat.

2.2.4. Characterization of starch-based gels after the 3D food printing

The images of the formulations were taken in a ScanCube® coupled with a camera (Canon EOS 750D®). The illumination and angle were adjusted and fixed for all formulations to standardize the images.

The texture profile analysis (TPA) of the 3D-printed cylinders was performed using a texture analyzer (TA. HD.plus, Stable Micro Systems Ltd, Godalming, Surrey, UK), and the 3D-printed cylinders were submitted to two compression cycles, using a 40 mm diameter compression plate geometry (P/35, Stable Micro System Ltd., Godalming, UK). The test conditions set were pre-test speed, test speed, and post-test speed of 1.00 mm s^{-1}, 2.00 mm s^{-1}, and 2.00 mm s^{-1}, respectively. The first compression distance was 5 mm, and the second was 10 mm, equivalent to a compression of 50 % of its original height. The time between the first and second compressions was 5 s. TPA was performed at a room temperature of 20°C and with five repetitions of each 3D-printed cylinder. The TPA parameters, according to Steffe (1996), were: hardness (force at maximum compression during a first bite); springiness (distance of compression cycle during the second bite); cohesiveness: (the area of work during the second bite divided by the area of work during the first bite); and gumminess (the product of hardness times cohesiveness). The TPA parameters were calculated from the force-time curve, using the OriginPro® 2020 Data Analysis and Graphing Software (OriginLab Corporation, Northampton, MA, USA).

2.2.5. Sensory evaluation of the 3D-printed cylinders

3D-printed cylinder sensory evaluation was performed using a descriptive sensory method, according to Mirazimi et al. (2023), with some modifications. The sensory evaluation was conducted over three sessions with ten recruited panelists (two males and eight females, aged between 20 and 60). In the first session, the project objectives were explained to the panelists, and the evaluation protocol was determined, including the definition of the six descriptors used in the sensory evaluation. This session was carried out using two 3D-printed cylinders for each panelist. The six descriptors defined by the panelists included in the

sensory evaluation were: viscosity, firmness, granularity, adhesiveness, dissolution speed, and persistence of a film in the mouth. Furthermore, the panelists were instructed at least one hour before the next sensory evaluation not to smoke, drink coffee, or consume any other food that could interfere with the sensory evaluation. Additionally, they were advised not to participate in the sensory evaluation if they had any illness that could affect the results. The second session consisted of training the panelists on the six descriptors and sensory evaluation protocols. In this session, all 3D-printed cylinders were offered to the panelists for intensity evaluation of the pre-defined descriptors. After the understanding of the second session, the protocol was individually verified to ensure good performance in the next session. In the third session, the 3D-printed cylinders were printed and organized according to Williams' Latin square experimental design. The 3D-printed cylinders were identified with a 3-digit code and presented simultaneously in trays to the panelists for comparative analysis of the six descriptors immediately after printing. The 3D-printed cylinders were analyzed in individual booths under red light to avoid interference at room temperature (20°C). Additionally, the panelists tasted approximately 0.5 g of each 3D-printed cylinder and rinsed their palates with drinking water between formulations. An unstructured 15-cm line scale (lower intensity on the left and higher intensity on the right) was used to quantify the descriptors described in Table 1. This study was approved by Paris-Saclay University's Research Ethics Committee (CER-PSCER-Paris-Saclay-2024-61). Before participation, the panelists signed the free informed consent and received a reward after the third session.

2.2.6. Statistical analyses

Except for sensory evaluation, all experiments were conducted in triplicate or more, and the data are presented as averages plus standard deviations. The data were evaluated by the Analysis of Variance (Multifactor ANOVA), applying Tukey's test ($p<0.05$) using the Statgraphics Centurion 19 software (StatPoint, Inc., USA).

Data from sensory analysis were submitted to an ANOVA using XLSTAT software for each attribute with products and panelists as main effects. Multiple pairwise comparisons were performed to interpret product differences (LSD test, $p<0.05$). A principal component analysis (PCA) was also performed to map 3D-printed cylinders according to their textural and rheological properties as principal variables and to sensory descriptors as explanatory variables.

3. Results and discussion

3.1. Characterization of the starch-based gels

The results of T_{mean} and T_{final} during 20 min of heating and pH of the starch-based gels are shown in Table 2. Maize had the T_{mean} significantly different from Wheat+kC, Tapioca and Tapioca+kC starch-based gels. The T_{final} did not show a significant difference among the starch-based gels, indicating that the thermal treatment was well standardized during the production of the starch-based gels. T_{mean} and T_{final} showed that for all starch-based gels, the production process occurred over the gelatinization temperature range expected in the literature for each botanical origin starch, such as for wheat (57.1 ± 0.3 – 66.2 ± 0.3) °C, maize (64.1 ± 0.2 – 74.9 ± 0.6) °C, tapioca (64.3 ± 0.1 – 74.4 ± 0.1) °C, and waxy (64.2 ± 0.2 – 74.6 ± 0.4) °C (Ai and Jane, 2015; Waterschoot et al., 2015).

Table 1
Sensory descriptors and definitions.

Parameters	Definitions
Viscosity	The sensation of thickness, the fluidness of the product, and the degree of the mass of food and saliva to hold the food together.
Firmness	The force that is required to compress the food between the tongue and the upper palate.
Granularity	The sensation of grains or particles between the tongue and the upper palate.
Adhesiveness	The stickiness of the food in the mouth.
Dissolution speed	The rate of the food is broken down in the mouth without chewing action.
Persistence of a film in the mouth	The sensation of the presence of the residual film in the mouth.

Table 2
Gelatinization temperatures (T_{mean} and T_{final}), and pH of the starch-based gels, during 20 min of heating.

Starch-based gels	T_{mean} (°C)	T_{final} (°C)	pH
Wheat	$77.2^{abB} \pm 2.0$	$83.4^{aA} \pm 1.0$	$3.12^{aA} \pm 0.01$
Wheat+kC	$75.3^{aA} \pm 1.0$	$84.1^{aA} \pm 0.8$	$3.18^{abAB} \pm 0.06$
Maize	$78.9^{bB} \pm 0.4$	$84.5^{aA} \pm 1.0$	$3.23^{abB} \pm 0.01$
Maize+kC	$78.0^{bB} \pm 0.7$	$84.6^{aA} \pm 0.6$	$3.09^{aA} \pm 0.04$
Tapioca	$76.5^{aA} \pm 0.9$	$83.4^{aA} \pm 1.4$	$3.35^{bB} \pm 0.03$
Tapioca+kC	$75.0^{aA} \pm 1.0$	$82.5^{aA} \pm 2.2$	$3.18^{abAB} \pm 0.04$
Waxy	$77.3^{abB} \pm 1.9$	$84.9^{aA} \pm 1.9$	$3.2^{aB} \pm 0.01$
Waxy+KC	$77.6^{bB} \pm 1.1$	$85.5^{aA} \pm 1.0$	$3.27^{bB} \pm 0.04$

Means with different letters in the column are significantly different ($p<0.05$) by Tukey's test: lowercase letters refer to significant differences between the starch sources, capital letters refer to significant differences due to the KC presence for each starch source.

In general, the pH of the gels with KC decreased due to the acid addition as expected (Table 2). The temperature, time, and shear rate during the production of starch-based gels lead to gelatinization and the total rupture of granules for Wheat (Fig. 1), with almost no granules remaining for Wheat+KC (Fig. 1). As for the other studied starch-based gels, after the gelatinization process, the presence of the Malta Cross in the polarized light images of the starch granules indicates incomplete gelatinization of the starch granules. All starch-based gels reached 75 °C in 5 min during thermal treatment, indicating that the presence of remaining granules was not due to temperatures below their gelatinization point.

3.1.1. Rheological properties of starch-based gels and their printability

The process in 3D extrusion-based printing generates high pressure and mechanical shear forces on starch-based gels, primarily influenced by their apparent viscosity and the requirement to exceed yield stress (Rong et al., 2023; Yang et al., 2018). As a result, all the starch-based gels that contained 15 g/100 g of starch could be extruded, but only the Wheat, Wheat+KC, Maize, and Maize+KC were able to form and maintain the structural integrity of layers (printable starch-based gels, Fig. 2A). In contrast, Tapioca, Tapioca+KC, Waxy, and Waxy+KC did not create and self-support in layers (non-printable starch-based gels, Fig. 2B).

The apparent viscosity of the printable (Fig. 2A) and non-printable (Fig. 2B) starch-based gels decreased with increasing shear rate, indicating that all starch-based gels exhibited a shear-thinning behavior. This behavior benefited the formulation extrusion through a thin nozzle in 3D extrusion-based printing (Yang et al., 2018). Printable starch-based gels showed similar behavior, leading to comparable values of consistency coefficient (K) and flow behavior index (n), depending on the starch source (Table 3). Starch-based gels on waxy were not printable, and it was not possible to obtain a good fit of the rheological data.

Carrageenans are used in food systems due to their ability to form gels. In a hot solution, the carrageenan molecules are in a coiled state. As the solution is cooled, they bind together in double-helical structures until they reach a state where the double helices entangle together with the ions' support (Fennema, 1996). In this study, the KC addition to printable starch-based gels leads to a slight decrease in apparent viscosity, and, consequently, the value of K. This effect was more pronounced in Maize+KC than in Wheat+KC (Table 3).

In the literature, many studies on a binary starch/carrageenan mixture explain the possible effects on starch characteristics due to the

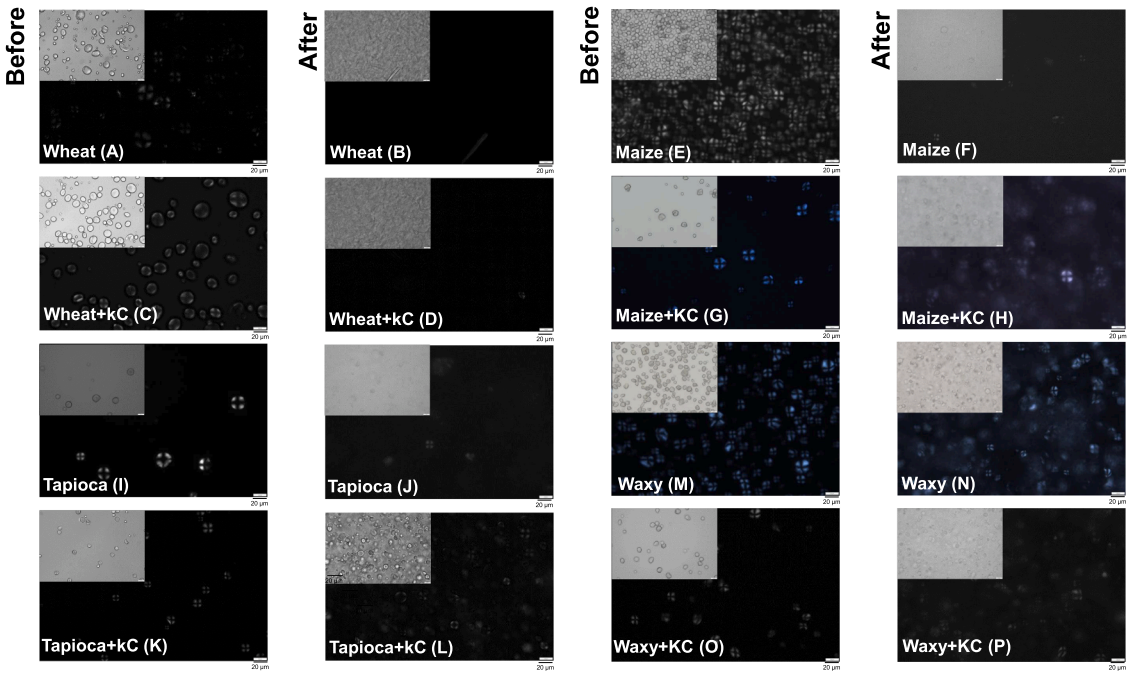

Fig. 1. Morphology of the starch suspension before gelatinization, and the starch-based gels after gelatinization: Wheat (A, B), Wheat+KC (C, D), Maize (E, F), and Maize+KC (G, H), Tapioca (I, J), Tapioca+KC (K, L), Waxy (M, N), and Waxy+KC (O, P), using both nonpolarized and polarized light, under 40 × magnification. The scale bar is 20 μm for all images.

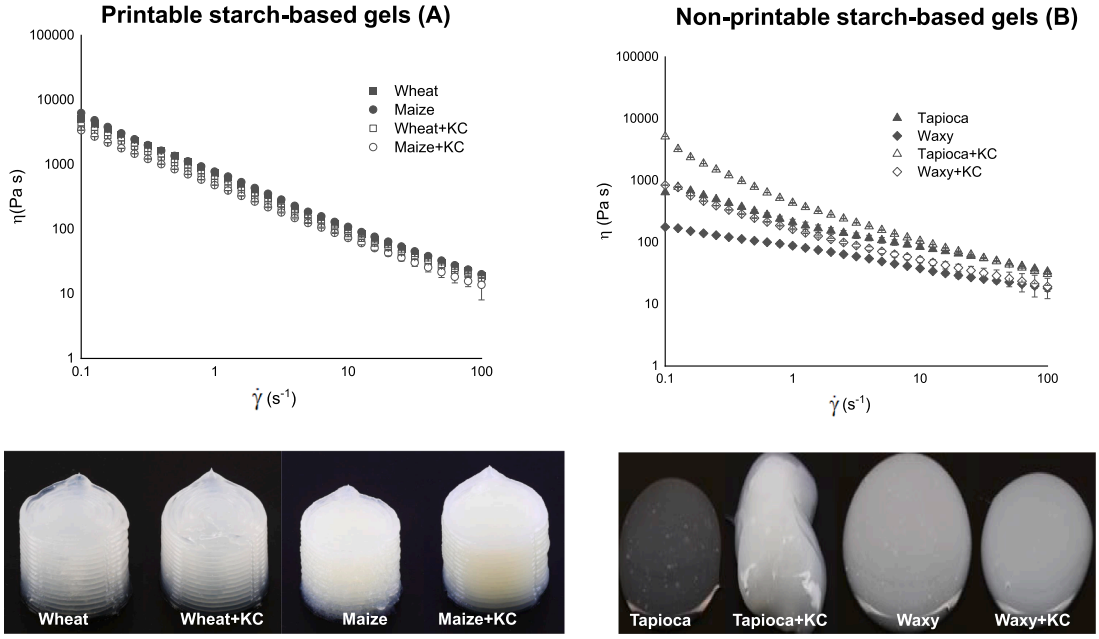

Fig. 2. Images and apparent viscosity of printable starch-based gels (A) and non-printable starch-based gels (B).

presence of carrageenans, such as gelatinization temperature, the granule sizes achieved after pasting, or the amount of leached molecules during pasting (Appelqvist et al., 1996; Appelqvist and Debet, 1997; Funami et al., 2008; Kim and BeMiller, 2012; Loisel et al., 2000; Nagano et al., 2008). Concerning viscosity measured with the Rapid Visco Analyzer, some studies found at the end of pasting, the viscosity values varied in increase or decrease with the KC presence (Funami et al., 2008; Kim and BeMiller, 2012; Tye, 1988), but all of them highlight particular behaviors, suggesting interaction mechanisms. For example, Savary et al. (2008) demonstrated by confocal laser microscopy that carrageenan penetrated starch granules or was adsorbed, as shown by Espinosa-Dzib et al. (2012), or even both mechanisms. The polysaccharides act as a "barrier'' or "film'', controlling the surface through adsorption and coating around the starch granules (Christianson, 1982; Funami et al., 2008), preventing abrasions between the granules and/or leaching of some starch molecules from the granules, both mechanisms that contribute to increasing the viscosity. The comparison of Maize and Maize+KC suggests that the coating capacity of KC inhibited the leaching of amylose in Maize+KC and acted as a lubricant, reducing abrasions between the granules; both effects led to a decrease in apparent viscosity in the continuous phase. Furthermore, comparing Maize with Maize + KC (Fig. 1), the last showed less disruption of the

Table 3
Rheological parameters obtained after data adjustment to Herschel-Bulkley model, shear storage modulus ($G^{'}$), shear loss modulus ($G^{''}$), and Tan delta (Tan δ) obtained from rheological measurements on starch-based gels.

Starch-based gels	τ_0 (Pa)	K (Pa s^n)	N (-)	R^2	$G^{'}$ (Pa)	$G^{''}$ (Pa)	Tan δ (-)	Printability	Stickiness (N)
Wheat	513.75	170.58	0.45	0.9943	4422	853	0.19	YES	10.11 ± 0.33^{bA}
Wheat+kC	409.93	154.47	0.46	0.9944	3938	869	0.22	YES	9.87 ± 0.11^{bA}
Maize	519.78	229.10	0.41	0.9961	5085	723	0.14	YES	8.07 ± 0.36^{abA}
Maize+kC	255.85	207.55	0.36	0.9977	3753	547	0.15	YES	7.72 ± 0.14^{abA}
Tapioca	13.07	210.07	0.61	0.9994	187	182	0.97	NO	15.42 ± 0.56^{cB}
Tapioca+kC	288.03	201.29	0.57	0.9969	302	252	0.84	NO	5.39 ± 0.07^{aA}
Waxy	-	-	-	-	98	112	1.14	NO	23.21 ± 0.7^{dD}
Waxy+KC	-	-	-	-	135	130	0.96	NO	15.37 ± 0.27^{cC}

[a] Herschel-Bulkley model: $\tau = \tau_0 + K\dot{\gamma}^n$

Means with different letters in the column are significantly different ($p<0.05$) by Tukey's test: lowercase letters refer to significant differences between the starch sources, capital letters refer to significant differences due to the KC presence for each starch source.

structure of the granules, represented by the presence of granule birefringence, indicating that KC could have acted as a coating on the starch granules, restricting the diffusion and absorption in the starch granules, thus avoiding the leaching of amylose.

Another mechanism described in the literature is the partial or total exclusion of hydrocolloids by starch granules during their swelling. The authors attributed this phenomenon to thermodynamic incompatibilities between starch granules and hydrocolloids (Alloncle et al., 1989; Annable et al., 1994; Matignon et al., 2014a). About Wheat and Wheat+KC, in Fig. 1, it showed total or partial rupture of the granule structure, without birefringence of the granules. A possible explanation for the Wheat and Wheat+KC showed a less pronounced decrease in apparent viscosity compared to the Maize and Maize+KC may be due to the exclusion phenomenon of swollen starch granules or the partial/total penetration of carrageenan into the wheat granules, of which both effects did not interfere with the gelatinization process.

The non-printable starch-based gels produced with tapioca starch showed higher n values, indicating less shear-thinning behavior (Table 3). Amylose-amylopectin ratio affects the 3D printability (Cheng et al., 2024b). Tapioca and waxy maize starches have between 17% and < 2% of amylose, respectively, lower than the 28% contained in maize and wheat starches (Fennema, 1996). The non-printable starch-based gels occurred probably due to highly branched amylopectin content, which was not effective in forming entanglements compared to gel formulations with high amylose content (Cheng et al., 2024b; Willett et al., 1997; Yu and Christie, 2005). Cheng et al. (2024b) evaluated maize starch with different amylose/amylopectin ratios, including waxy maize starch with a ratio of (2:98). They concluded that, due to the presence of amylopectin, although the starch gel presented continuous extrusion performance and good adhesiveness, it was inefficient in its printing support capacity, making it unfavorable for 3D food processing.

As a result of this study, the tapioca and waxy starches did not provide any structure, and the formulations directly accumulated in a circular shape (Fig. 2B). Another possibility of this 3D food printing low performance was the presence of glucose+maltodextrin in these formulations, without effective entanglements in the Tapioca+KC and Waxy+KC, the free water was more available to bind with the glucose and maltodextrin, reducing the gel strength (Ai and Jane, 2015). Fig. 1 also suggests the influence of the glucose+maltodextrin presence. Tapioca and Waxy showed large amounts of birefringent granules, indicating that water was not free to diffuse and absorb into the starch granules.

The KC presence in the non-printable starch-based gels increased the apparent viscosity, showing a more pronounced shear-thinning effect (Table 3), probably due to the KC's ability to form gels. Nevertheless, for the tapioca and waxy maize starch formulations, this effect was not sufficient to have enough structure to form the layers.

3.1.2. *Self-supporting of starch-based gels*

The shear stress produced by a sinusoidal strain results in the shear storage modulus ($G^{'}$) and the shear loss modulus ($G^{''}$) (Steffe, 1996), both components are relevant to study the self-supporting stage of 3D food printing, as the formulations themselves need to have sufficient mechanical strength to maintain their structural stability. $G^{'}$ reflects the mechanical strength of the formulations, up to a certain point. The higher its value, the more favorable the formulation's self-supporting performance (Cheng et al., 2024b; Zhang et al., 2024; Zhang et al., 2023). In contrast, $G^{''}$ represents dissipated energy, related to viscosity or fluid-like behavior. Fig. 3 shows the oscillation amplitude sweeps of the printable and non-printable starch-based gels. All printable starch-based gels exhibit $G^{'}>G^{''}$ at a constant deformation of 1% strain, indicating solid-like behavior at the low shear strain produced, which is beneficial for the 3D form stability, and fluid-like behavior above the yield stress.

The highest $G^{'}$ value was for Maize, followed by Wheat, > Wheat+KC, and > Maize+KC (Table 3). The results indicated that Maize exhibits the highest solid-like behavior among the starch-based gel formulations, suggesting that it had the highest support performance in 3D food printing (Cheng et al., 2024b). These results corroborate with the apparent viscosity behavior, which is also more pronounced in Maize and Maize+KC than in Wheat and Wheat+KC, as already discussed (Section 3.1.1). In addition, Cheng et al. (2024b) and Xie et al. (2009) reported that the leached amylose produced effective entanglements that increase the solid-like behavior of the starch gel.

The highest fluid-like behavior ($G^{''}$) was for Waxy, followed by >Waxy+KC, >Tapioca, and >Tapioca+KC, resulting in non-printable

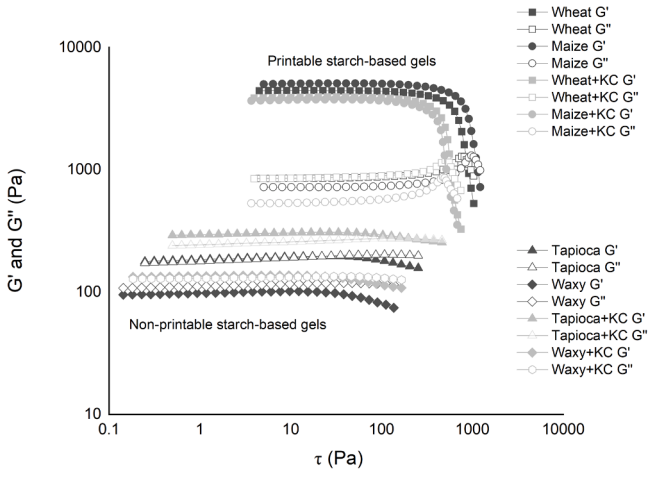

Fig. 3. Representative oscillation amplitude sweeps for printable and non-printable starch-based gels.

starch-based gels, showing that it had no support performance in 3D food printing (Fig. 2B). The addition of KC addition increased the solid-like behavior (Waxy+KC and Tapioca+KC), probably due to the ability of carrageenan to form gels; however, it is not sufficient for 3D printing.

Another common parameter to describe the formulation's visco-elastic behavior is the tangent of the phase shift or phase angle (Tan δ), which can indicate the structuration of the matrix state. For the printable starch-based gels, Tan δ was < 1, ranging between (0.14 – 0.22), indicating high structuration. In contrast, the non-printable starch-based gels (Tapioca, Tapioca+KC, and Waxy+KC) Tan δ ranged between (0.84 – 0.97), in which Tapioca+KC and Waxy+KC demonstrated solid-like behavior, but were not sufficient to allow the formulations to keep their shape after printing. For Waxy, which behaved as fluid-like, Tan δ was >1 (1.14) and did not retain its shape after printing. Azam et al. (2018) studied the effect of different hydrocolloids on the 3D printing of vitamin-D enriched orange concentrate wheat starch formulations, and they found Tan δ values less than 1 for all formulations, indicating their dominant elastic behavior. Masbernat et al. (2021) studied the printability of wheat flour-based products and concluded that formulations with Tan δ in the range (0.14 – 0.17) presented the best printing quality. Similar studies on 3D food printing have found Tan δ values <1, also indicating its predominantly elastic behavior (Chen et al., 2019; Yang et al., 2021; Yang et al., 2018).

3.1.3. Shear recovery of starch-based gels

As mentioned, extrusion in 3D extrusion-based printing exerts a shear force on the starch-based gels to ensure their effective flow through the nozzle. The recovery test of printable and non-printable starch-based gels was performed to reproduce the shear conditions during extrusion printing and to verify the starch-based gel's recovery ability after the 3D extrusion-based printing process. In Fig. 4A, the solid behavior of the printable starch-based gels recovers immediately after high shear, as demonstrated by the considerable gap between G' and G''. These results confirm the solid-like behavior for all printable starch-based gels, which were also able to be extruded and rapidly recovered of G' after the high shear applied, having sufficient mechanical strength to maintain and support the structural integrity of the layer and the next extruded layer (Liu et al., 2019).

The shear G' recovery ability values obtained in 30 s in the third step after a high shear rate applied for the Wheat, Maize, Wheat+KC, and Maize+KC were 27, 23, 23, and 31%, respectively, with the Maize+KC having the highest G' recovery ability among the formulations. The results also indicated that KC was coating the starch granules in Maize+KC, if compared to the G' recovery abilities (31% with KC, 23 % without). The rapid recovery of G' within 30 s in the third stage after a high shear rate can be related to the rapid reformation of the network, which was allowed by the partially restored conformation due to the reconstruction of the physically entangled structure (Chen et al., 2019; Winnik and Yekta, 1997). Shaw (2012) suggested the polymer conformational change theory, which states that the polymer system's conformational entropy reduction is due to the macromolecular chains being oriented along the flow direction under external stress. After removing the applied stress, part of the conformational entropy is restored.

For the Wheat and Wheat+KC, there was a decrease from 27 % to 23 % in their G' recovery ability, again suggesting that the KC was partially/fully penetrated in the wheat granules, which did not contribute to the formation of the network and, consequently, was not present to be restored.

For Tapioca, Tapioca+KC, and Waxy+KC starch-based gels, the solid behavior did not recover immediately after high shear, as demonstrated by the small gap between G' and G'', and the prevalence of liquid-like behavior (Fig. 4B). Waxy showed the prevalence of liquid-like behavior throughout the test. Thus, the non-printable starch-based gels continued to flow after the shear rate was applied, confirming that they could not form and maintain the structural integrity of layers (Fig. 2B).

3.1.4. 3D Printing performance and stickiness behavior

The 3D-printed cylinder appearance was used to characterize the starch-based gel printing performance. All 3D-printed cylinders (Fig. 2A) showed bright and good structural stability without collapsing, exhibiting acceptable printing performance. 3D-printed cylinders with KC lead to an increase in the appearance of well-defined layers. The rougher surface of Maize is probably due to the absence of KC. In addition, Maize and Maize+KC showed a yellowing tendency than Wheat and Wheat+KC, probably due to the presence of yellow pigments such as lutein (BeMiller and Whistler, 2009; Larrea-Wachtendorff et al., 2021). The Wheat+KC showed a failure in the surface layer related to discontinuous extrusion, which generally results in broken extruded threads (Cheng et al., 2024a).

Stickiness is a relevant sensory attribute of semi-solid food (Dunnewind et al., 2004; Weenen et al., 2003), which was defined by Jowitt (1974) as "Possessing the textural property manifested by a

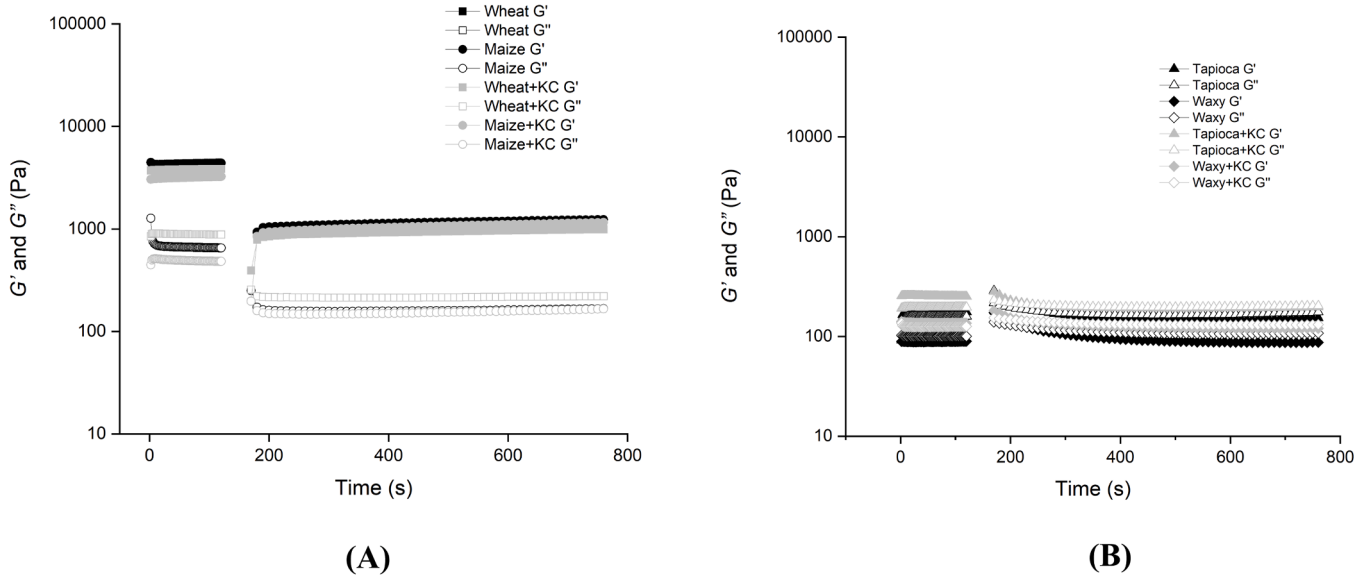

Fig. 4. Recovery test of printable (A) and non-printable starch-based gels (B) after applying the maximum high shear rate.

tendency to adhere to contacting surfaces, especially the palate, teeth, and tongue during mastication" and depends on adhesive and cohesive properties (Burke and Hartel, 2021; Noren et al., 2019).

For the printable starch-based gels, it was observed that adhesive-cohesive failure occurred with cohesive dominance. After complete separation (formulation – probe), the formulation residue covers a large part of the probe surface (Adhikari et al., 2003). The Maize and Maize+KC stickiness was (8.07 ± 0.36 N and 7.72 ± 0.14 N) lower than Wheat and Wheat+KC (10.11 ± 0.33 N and 9.87 ± 0.11 N), being significantly different depending on the starch origin, as shown in Table 3. The presence of KC led to a slight decrease in the stickiness of both starches, but without a significant difference.

In addition, the printable starch-based gel cohesive domain was probably highly influenced by the glucose-maltodextrin solution. Adhikari et al (2003) studied the stickiness characterization of sugar-rich foods and found that maltodextrin presence in a sugar solution increased the cohesive strength.

In general, non-printable starch-based gels showed higher stickiness values, with Waxy having the highest value (Table 3). Similarly, stickiness values decreased in all formulations in the presence of KC. Li et al. (2017) and Ayabe et al. (2009) also studied the textural properties and rice starch structures and demonstrated that stickiness increases with leached amylopectin content. The study suggested that an increase in the amount of amylopectin led to a higher proportion of short amylopectin chains and smaller amylopectin molecular sizes, favoring bonding and molecular interactions, and consequently increasing stickiness. Thus, the higher stickiness values demonstrated by the non-printable starch-based gels are probably due to their high amylopectin content.

Therefore, from this point on in the study, only the printable starch-based gels in 3D-printed cylinder form were used in the next analyses.

3.2. Characterization of starch-based gels after the 3D food printing

Food texture is considered in many aspects of sensory properties and it is influenced by food structure, rheology, and surface properties (Kravchuk et al., 2012; Stokes et al., 2013). The texture profiles obtained from the 3D-printed cylinders, including hardness, springiness, and gumminess, are shown in Table 4. The hardness indicates the force required for the deformation of the product (He et al., 2020). In addition, gumminess refers to the energy needed to rupture the semi-solid formulation into a stable state, allowing it to be swallowed (Hurler et al., 2012; Yang et al., 2018). The KC presence decreased the hardness and gumminess of the 3D-printed cylinders, showing significant differences for both starches. This result corroborated the rheological properties of printable starch-based gels, which showed that adding KC leads to a slight decrease in apparent viscosity and $G^{`}$, which consequently decreases the mechanical strength of the Wheat+KC and Maize+KC.

Springiness indicates elasticity (the ability of a formulation to revert to its original form after deformation) (Yang et al., 2018). All 3D-printed cylinders did not show significant differences in springiness. A possible reason for the absence of a difference in springiness is that the 3D-printed cylinders were produced and immediately TPA was performed, not allowing significant water loss or starch retrogradation effects. The cohesiveness of the 3D-printed cylinders based on wheat was slightly lower relative to the 3D-printed cylinders based on maize.

Table 4
Hardness, cohesiveness, springiness and gumminess obtained from Texture profile analysis (TPA) of the 3D-printed cylinders, from only the printable starch-based gels.

Starch-based gels	Hardness (N)	Cohesiveness	Springiness (mm)	Gumminess (N)
Wheat	1.02^{bB} ± 0.02	2.29^{aA} ± 0.03	9.94^{aA} ± 0.05	2.30^{bB} ± 0.02
Wheat+kC	0.65^{aA} ± 0.01	2.33^{aA} ± 0.01	9.95^{aA} ± 0.04	1.52^{aA} ± 0.01
Maize	1.02^{bB} ± 0.01	2.39^{aA} ± 0.02	9.95^{aA} ± 0.01	2.37^{bB} ± 0.12
Maize+kC	0.62^{aA} ± 0.01	2.54^{aA} ± 0.08	9.93^{aA} ± 0.09	1.57^{aA} ± 0.07

Means with different letters in the column are significantly different ($p<0.05$) by Tukey's test: lowercase letters refer to significant differences between the starch sources, capital letters refer to significant differences due to the KC presence for each starch source.

3.3. Sensory evaluation of 3D-printed cylinders

In this study, sensory evaluation was conducted with ten panelists to evaluate the 3D-printed cylinders according to the definition of sensory descriptors presented in Table 1. Fig. 5 shows the overall mean intensity of each formulation perceived by the panelists. Adding thickeners affects the food texture, allowing for differences in sensory perception (Peh et al., 2022; Sharma et al., 2017). Generally, foods containing thickeners were perceived to have greater firmness and stickiness in the mouth and throat attributes (Peh et al., 2022). The opposite behavior was found in this study; 3D-printed cylinders of Wheat and Maize were perceived to be significantly more viscous, firmer, and adhesive in the mouth compared to Wheat+KC and Maize+KC.

Firmness can be associated with viscosity, which is defined as the sensation of thickness, the fluidness of the product, and the degree to which the mass of food and saliva hold the food together. It has been suggested that the more viscous a product is, the more force will be needed to compress the food (Ballou Stahlman et al., 2000). The descriptors of firmness and viscosity perceived by panelists corroborate the instrumental behaviors of this study (rheology and TPA).

Adhesiveness is attributed to the stickiness of food in the mouth, and it may be related to the difficulty of swallowing. A more adhesive food would be more difficult to swallow (Peh et al., 2022; Steele et al., 2015). When comparing the sensorial evaluation with instrumental stickiness measurement, adding the KC allows for decreased perception of adhesiveness, and Maize+KC was perceived to have less adhesiveness in the mouth.

3D-printed cylinders made from maize starch are perceived to show more graininess than 3D-printed cylinders made from wheat starch. Certainly, the morphology showed total rupture of the granules for Wheat, with almost no remaining granules for Wheat and Wheat+KC (Fig. 1B and 1D). The highest granularity value was for Maize+KC, also corroborating with its morphology (Fig. 1).

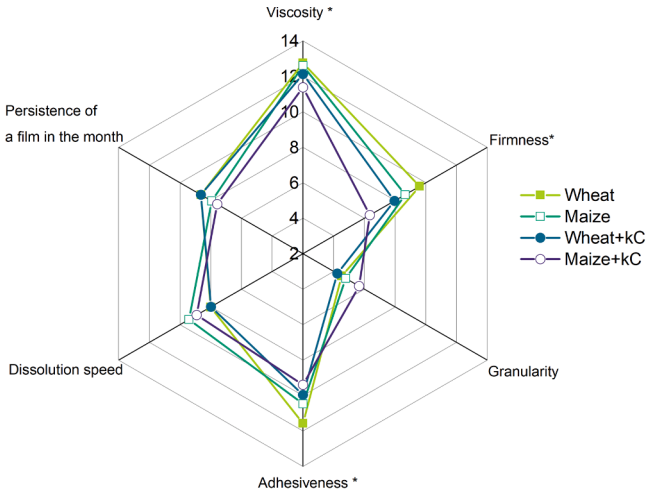

Fig. 5. The sensory analysis descriptors revealed significant differences in the ANOVA test, with multiple pairwise comparisons (LSD), indicated by an asterisk (*).

Similar behaviors were observed for the dissolving speed descriptor, which was considered the rate at which food is broken down in the mouth without chewing action. The highest dissolving speed values were for the 3D-printed cylinders made from maize starch, which means that these 3D-printed cylinders were more difficult to deform and disintegrate when subjected to a force applied between the tongue and the upper palate in the mouth. Regarding the sensation of presence of the residual film in the presence of mouth, the KC influenced the formulations. Wheat and Maize are perceived to provide more residual film in the mouth compared to Wheat+KC and Maize+KC; this could be attributed to the KC thickener effect, which provided a coating layer between the tongue and palate, giving less starch residual film in the mouth perception (Peh et al., 2022).

The sensory evaluation of texture was a challenge for the 3D-printed cylinders. However, the sensory analysis showed the primary texture perceptions of the 3D-printed cylinders, which is particularly useful for determining the main differentiation criteria. Thus, more evaluation sessions and additional training for the panelists to increase their ability to differentiate textures.

3.4. The link between sensory evaluation, apparent viscosity, and texture properties by instrumental measurements of 3D-printed cylinders

The interaction between instrumental texture properties, apparent viscosity, and sensory evaluation is an interesting strategy for understanding the complexity of food texture (Sharma et al., 2017; van Vliet, 2002). Principal component analysis (Fig. 6A) was performed to map 3D-printed cylinders (Fig. 6B) to understand the behavior of 3D-printed cylinders' textures between the instrumental measurements, rheology, and texture analysis (dependent and principal variables), and sensory evaluation (independent and explanatory variables). Principal components 1 and 2 explain 91.47% of the total variance. Component 1 explained 51.94% of the 3D-printed cylinder texture properties, demonstrating the link between instrumental measurements and sensory evaluation. However, only the hardness of the TPA parameters obtained in the 3D-printed cylinders showed correlations with the firmness of the sensory evaluation and could be distinguished in component 1. The PCA map (Fig. 6B) reveals that the Wheat was firmer. In contrast, Maize+KC showed a negative correlation, which provided to be the least firm of all the formulations. This result can be extended to gumminess, as it can be related to the energy needed to rupture the semi-solid formulation. Stickiness was not correlated with adhesiveness in component 1, but it could be complementary results, indicating that Wheat showed more adhesive/sticky behavior and Maize+KC showed the opposite behavior. The viscosity of the rheological result was supported by component 2 (39.53%) and was not correlated with the viscosity of the sensorial values. The absence of correlation may be due to the viscosity measured in the rheometer reflecting the flow behavior under highly controlled conditions, while sensory values involve more complex and subjective human factors. However, the rheological results complement the sensory values, supporting that the presence of KC leads to a decrease in viscosity.

4. Conclusions

This study showed that starch-based gels produced with wheat and maize, with or without KC, were successfully printed using 3D extrusion-based printing. The presence of KC in printable starch-based gels leads to a slight decrease in apparent viscosity. The starch-based gels based on tapioca and waxy starch were not printable, probably because of the high amylopectin content. Sensory evaluation showed that the addition of KC allowed differences in sensory perception. Wheat and Maize were perceived to be significantly more viscous, firmer, and adhesive in the mouth compared to Wheat+KC and Maize+KC. It was possible to link sensory evaluation and instrumental measurements of 3D-printed cylinders. The hardness of the TPA parameters showed a correlation with the firmness of the sensory evaluation, demonstrating that the Wheat was firmer. In contrast, Maize+KC showed to be the least firm of all the formulations.

Thus, this study showed the importance of rheological properties in the printability of starch-based gels, as well as the link between printability, instrumental analyses, and sensory evaluation. The starch source influenced the printability and ability to form and maintain the structural integrity of the layers. The addition of KC affected the rheological properties and texture, which could be perceived through sensory analysis.

CRediT authorship contribution statement

Taíse Toniazzo: Writing – review & editing, Writing – original draft, Methodology, Investigation, Formal analysis, Data curation, Conceptualization. **Cassandre Leverrier:** Writing – review & editing, Supervision, Conceptualization. **Nathália Lisboa Souza:** Methodology, Investigation, Data curation. **Giana Almeida:** Writing – review & editing, Supervision, Conceptualization. **Carmen Cecília Tadini:** Writing – review & editing, Supervision, Funding acquisition, Conceptualization. **Valérie Guenard-Lampron:** Writing – review & editing, Supervision, Conceptualization.

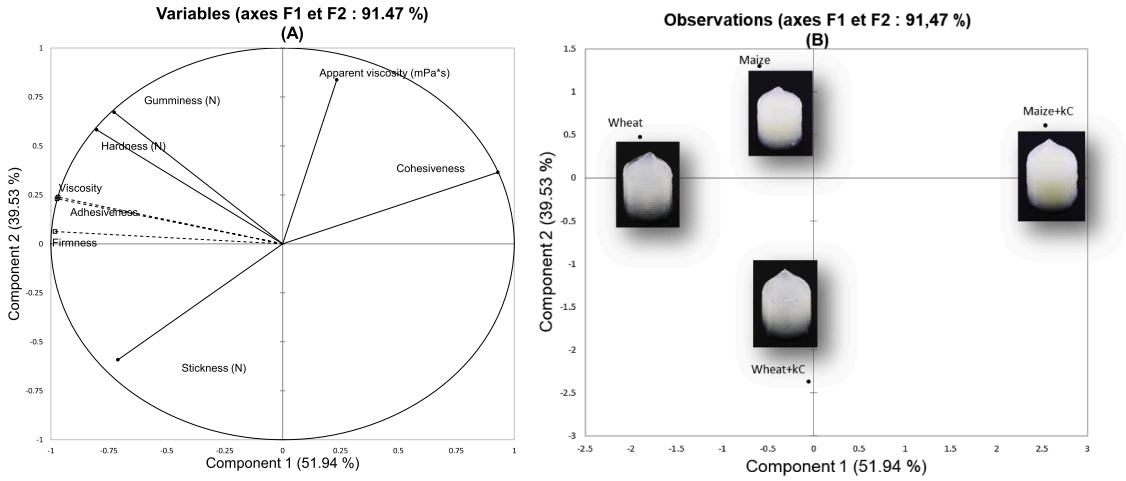

Fig. 6. Principal component analysis showing the variation between textural and rheological properties (loading plot) (A) and 3D-printed cylinder formulations (score plot) (B). Principal variables were from textural and rheological properties (straight lines), and explanatory variables were from sensory properties (discontinuous lines).

Declaration of competing interest

The authors declare that they have no known competing financial interests or personal relationships that could have appeared to influence the work reported in this paper.

Acknowledgments

Funding: The authors are grateful to the Coordination for the Improvement of Higher Education Personnel (CAPES) for supporting this study [grant numbers 88887.899092/2023-00. 88881.712038/2022-01], regarding the approved program CAPES-COFECUB, and from the National Council for Scientific and Technological Development (CNPq) under grant 309548/2021-7. The funding sources had no involvement in the study design, data collection, analyses, and interpretation of data, or in the decision to submit this article for publication. The authors would like to thank AgroParisTech, UMR SayFood, and especially the IHAC and GéPro groups, for hosting and all supporting needed during the internship; Ms. Julio Henrique Santiago Formiga Ramos for providing the cylinder format in STL files for the 3D food printing; for Cargill for donating the starches, maltodextrin, and carrageenan.

Data availability

Data will be made available on request.

References

Achayuthakan, P., Suphantharika, M., 2008. Pasting and rheological properties of waxy corn starch as affected by guar gum and xanthan gum. Carbohydr. Polym. 71 (1), 9–17.
Adhikari, B., Howes, T., Bhandari, B., Truong, V., 2003. In situ characterization of stickiness of sugar-rich foods using a linear actuator driven stickiness testing device. J. Food Eng. 58 (1), 11–22.
Ai, Y., Jane, J.I., 2015. Gelatinization and rheological properties of starch. Starch-Stärke 67 (3-4), 213–224.
Alloncle, M., Lefebvre, J., Llamas, G., Doublier, J., 1989. A rheological characterization of cereal starch-galactomannan mixtures. Cereal. Chem. 66 (2), 90–93.
Annable, P., Fitton, M., Harris, B., Phillips, G., Williams, P., 1994. Phase behaviour and rheology of mixed polymer systems containing starch. Food Hydrocoll. 8 (3-4), 351–359.
Appelqvist, I., Brown, C., Goff, T., Lane, S., Norton, I., 1996. Application of hydrocolloids in frozen sauces. In: Phillips, G.O., Williams, P.A., Wedlock, D.J. (Eds.), Gums and Stabilizers for the Food Industry, Gums and Stabilizers for the Food Industry, 8. IRL Press, Oxford.
Appelqvist, I.A.M., Debet, M., 1997. Starch-biopolymer interactions—A review. Food Rev. Int. 13, 163–224.
Ayabe, S., Kasai, M., Ohishi, K., Hatae, K., 2009. Textural properties and structures of starches from indica and japonica rice with similar amylose content. Food Sci. Technol. Res. 15 (3), 299–306.
Azam, R.S., Zhang, M., Bhandari, B., Yang, C., 2018. Effect of different gums on features of 3D printed object based on vitamin-D enriched orange concentrate. Food Biophys. 13, 250–262.
Ballou Stahlman, L., Mertz Garcia, J., Hakel, M., Chambers IV, E., 2000. Comparison ratings of pureed versus molded fruits: preliminary results. Dysphagia 15, 2–5.
BeMiller, J.N., Whistler, R.L., 2009. Starch: chemistry and technology. Academic Press.
Bitencourt, B.S., Guedes, J.S., Saliba, A., Sartori, A.G.O., Torres, L.C.R., Amaral, J., Alencar, S.M., Maniglia, B.C., Augusto, P.E.D., 2023. Mineral bioaccessibility in 3D printed gels based on milk/starch/& kappa;-carrageenan for dysphagic people. Food Res. Int. 170. https://doi.org/10.1016/j.foodres.2023.113010.
Burke, J., Hartel, R., 2021. Stickiness of sugar syrups with and without particles. J. Food Eng. 290, 110222.
Campo, V.L., Kawano, D.F., da Silva Jr, D.B., Carvalho, I., 2009. Carrageenans: biological properties, chemical modifications and structural analysis–A review. Carbohydr. Polym. 77 (2), 167–180.
Chen, H., Xie, F., Chen, L., Zheng, B., 2019. Effect of rheological properties of potato, rice and corn starches on their hot-extrusion 3D printing behaviors. J. Food Eng. 244, 150–158.
Cheng, Y., Gao, W., Kang, X., Wang, J., Yu, B., Guo, L., Zhao, M., Yuan, C., Cui, B., 2024a. Effects of starch–fatty acid complexes with different fatty acid chain lengths and degrees of saturation on the rheological and 3D printing properties of corn starch. Food Chem. 436, 137718.
Cheng, Y., Liang, K., Chen, Y., Gao, W., Kang, X., Li, T., Cui, B., 2023. Effect of molecular structure changes during starch gelatinization on its rheological and 3D printing properties. Food Hydrocoll. 137, 108364.
Cheng, Y., Yuqing, H., Xiao, L., Gao, W., Kang, X., Sui, J., Cui, B., 2024b. Impact of starch amylose and amylopectin on the rheological and 3D printing properties of corn starch. Int. J. Biol. Macromol. 278, 134403.
Chow, C., Thybo, C., Sager, V., Riantiningtyas, R., Bredie, W., Ahrné, L., 2021. Printability, stability and sensory properties of protein-enriched 3D-printed lemon mousse for personalised in-between meals. Food Hydrocoll. 120. https://doi.org/10.1016/j.foodhyd.2021.106943.
Christianson, D., 1982. Hydrocolloid interactions with starches. Food Carbohydrates 399–419.
Cotabarren, I.M., De Salvo, M.I., Palla, C.A., 2023. Structuring food products using 3D printing: strategies, applications, and potential. Current Food Sci. Technol. Reports 1 (2), 109–121.
Cui, Y., Li, C., Guo, Y., Liu, X., Zhu, F., Liu, Z., Liu, X., Yang, F., 2022. Rheological & 3D printing properties of potato starch composite gels. J. Food Eng. 313, 110756.
Dunnewind, B., Janssen, A., Van Vliet, T., Weenen, H., 2004. Relative importance of cohesion and adhesion for sensory stickiness of semisolid foods. J. Texture Stud. 35 (6), 603–620.
Espinosa-Dzib, A., Ramírez-Gilly, M., Tecante, A., 2012. Viscoelastic behavior and microstructure of aqueous mixtures of cross-linked waxy maize starch, whey protein isolate and κ-carrageenan. Food Hydrocoll. 28 (2), 248–257.
Fennema, O.R., 1996. Food Chemistry. CRC Press.
Funami, T., Nakauma, M., Noda, S., Ishihara, S., Asai, I., Inouchi, N., Nishinari, K., 2008. Effects of some anionic polysaccharides on the gelatinization and retrogradation behaviors of wheat starch: soybean-soluble polysaccharide and gum arabic. Food Hydrocoll. 22 (8), 1528–1540.
Guedes, J., Bitencourt, B., Augusto, P., 2023. Modification of maize starch by dry heating treatment (DHT) and its use as gelling ingredients in fruit-based 3D-printed food for dysphagic people. Food Biosci. 56. https://doi.org/10.1016/j.fbio.2023.103310.
He, C., Zhang, M., Guo, C., 2020. 4D printing of mashed potato/purple sweet potato puree with spontaneous color change. Innovat. Food Sci. Emerg. Technol. 59, 102250.
Hurler, J., Engesland, A., Poorahmary Kermany, B., Škalko-Basnet, N., 2012. Improved texture analysis for hydrogel characterization: gel cohesiveness, adhesiveness, and hardness. J. Appl. Polym. Sci. 125 (1), 180–188.
Hussain, S., Malakar, S., Arora, V., 2022. Extrusion-based 3D food printing: technological approaches, material characteristics, printing stability, and post-processing. Food Eng. Rev. 14 (1), 100–119. https://doi.org/10.1007/s12393-021-09293-w.
Ji, S., Xu, T., Li, Y., Li, H., Zhong, Y., Lu, B., 2022. Effect of starch molecular structure on precision and texture properties of 3D printed products. Food Hydrocoll. 125, 107387.
Jowitt, R., 1974. The terminology of food texture. J. Texture Stud. 5 (3), 351–358.
Kim, H.-S., BeMiller, J.N., 2012. Effects of hydrocolloids on the pasting and paste properties of commercial pea starch. Carbohydr. Polym. 88 (4), 1164–1171.
Kozu, H., Kamata, T., Umeda, T., Nei, D., Kobayashi, I., 2025. Characterization of screw-based 3D food printing based on tensile strength of paste-type food inks. Food Bioproc. Tech. 18 (6), 5146–5163. https://doi.org/10.1007/s11947-024-03736-y.
Kravchuk, O., Torley, P., Stokes, J.R., 2012. Food texture is only partly rheology. Food Mater. Sci. Eng. 349–372.
Larrea-Wachtendorff, D., Sousa, I., Ferrari, G., 2021. Starch-based hydrogels produced by high-pressure processing (HPP): effect of the starch source and processing time. Food Eng. Rev. 13 (3), 622–633.
Lascombes, C., Agoda-Tandjawa, G., Boulenguer, P., Le Garnec, C., Gilles, M., Mauduit, S., Barey, P., Langendorff, V., 2017. Starch-carrageenan interactions in aqueous media: role of each polysaccharide chemical and macromolecular characteristics. Food Hydrocoll. 66, 176–189.
Leam, P.X.N., Pant, A., An, J., Leo, C.H., Tan, U.-X., Chua, C.K., 2024. A preliminary investigation on the effect of ingredient flow speed in extrusion-based printing through experimental and theoretical approaches. Int. J. Bioprint. 10 (5), 2787.
Li, H, Fitzgerald, MA, Prakash, S, Nicholson, TM, Gilbert, RG, 2017. The molecular structural features controlling stickiness in cooked rice, a major palatability determinant. Sci. Rep. 7 (1), 43713. https://doi.org/10.1038/srep43713.
Li, G., Zhan, J., Hu, Z., Huang, J., Luo, X., Chen, J., Yuan, C., Takaki, K., Hu, Y., 2022. 3D printing properties and printability definition of Pennahiaargentata surimi and rice starch. Food Biosci. 48, 101748.
Lille, M., Nurmela, A., Nordlund, E., Metsä-Kortelainen, S., Sozer, N., 2018. Applicability of protein and fiber-rich food materials in extrusion-based 3D printing. J. Food Eng. 220, 20–27. https://doi.org/10.1016/j.jfoodeng.2017.04.034.
Liu, B., Zhu, S., Zhong, F., Yokoyama, W., Huang, D., Li, Y., 2021. Modulating storage stability of binary gel by adjusting the ratios of starch and kappa-carrageenan. Carbohydr. Polym. 268, 118264.
Liu, Z., Bhandari, B., Prakash, S., Mantihal, S., Zhang, M., 2019. Linking rheology and printability of a multicomponent gel system of carrageenan-xanthan-starch in extrusion based additive manufacturing. Food. Hydrocoll. 87, 413–424.
Loisel, C., Cantoni, P., Tecante, A., Doublier, J., 2000. Effect of temperature on the rheological properties of starch/carrageenan mixtures. Gums and Stabilisers Food Industry 10, 181–187. Elsevier.
Mantihal, S., Prakash, S., Bhandari, B., 2019. Texture-modified 3D printed dark chocolate: sensory evaluation and consumer perception study. J. Texture Stud. 50 (5), 386–399. https://doi.org/10.1111/jtxs.12472.
Markovinovic, A., Bosiljkov, T., Janci, T., Kostic, M., Dedovic, N., Lucic, E., Bavrka, K., Pavlic, B., Kovacevic, D., 2024. Characterization of antioxidant bioactive compounds and rheological, color and sensory properties in 3D-printed fruit snacks. Foods. 13 (11). https://doi.org/10.3390/foods13111623.
Masbernat, L., Berland, S., Leverrier, C., Moulin, G., Michon, C., Almeida, G., 2021. Structuring wheat dough using a thermomechanical process, from liquid food to 3D-

printable food material. J. Food Eng. 310. https://doi.org/10.1016/j.jfoodeng.2021.110696.
Matignon, A., Barey, P., Desprairies, M., Mauduit, S., Sieffermann, J.-M., Michon, C., 2014a. Starch/carrageenan mixed systems: penetration in, adsorption on or exclusion of carrageenan chains by granules? Food Hydrocoll. 35, 597–605.
Matignon, A., Moulin, G., Barey, P., Desprairies, M., Mauduit, S., Sieffermann, J.-M., Michon, C., 2014b. Starch/carrageenan/milk proteins interactions studied using multiple staining and Confocal Laser Scanning Microscopy. Carbohydr. Polym. 99, 345–355.
Mirazimi, F., Saldo, J., Sepulcre, F., Pujolà, M., 2023. Study the correlation between the instrumental and sensory evaluation of 3D-printed protein-fortified potato puree. European Food Res. Technol. 249 (6), 1669–1675.
Nagano, T., Tamaki, E., Funami, T., 2008. Influence of guar gum on granule morphologies and rheological properties of maize starch. Carbohydr. Polym. 72 (1), 95–101.
Noren, N.E., Scanlon, M.G., Arntfield, S.D., 2019. Differentiating between tackiness and stickiness and their induction in foods. Trends. Food Sci. Technol. 88, 290–301.
Peh, J.X., Lim, W., Tha Goh, K.K., Dharmawan, J., 2022. Correlation between instrumental and sensory properties of texture-modified carrot puree. J. Texture Stud. 53 (1), 72–80.
Qiu, Y., McClements, D.J., Chen, J., Li, C., Liu, C., Dai, T., 2023. Construction of 3D printed meat analogs from plant-based proteins: improving the printing performance of soy protein-and gluten-based pastes facilitated by rice protein. Food Res. Int. 167, 112635.
Rayna, T., Striukova, L., 2016. From rapid prototyping to home fabrication: how 3D printing is changing business model innovation. Technol. Forecast. Soc. Change 102, 214–224. https://doi.org/10.1016/j.techfore.2015.07.023.
Ren, S., Tang, T., Bi, X., Liu, X., Xu, P., Che, Z., 2023. Effects of pea protein isolate on 3D printing performance, nutritional and sensory properties of mango pulp. Food Biosci. 55. https://doi.org/10.1016/j.fbio.2023.102994.
Riantiningtyas, R., Sager, V., Chow, C., Thybo, C., Bredie, W., Ahrne, L., 2021. 3D printing of a high protein yoghurt-based gel: effect of protein enrichment and gelatine on physical and sensory properties. Food Res. Int. 147. https://doi.org/10.1016/j.foodres.2021.110517.
Rochas, C., Rinaudo, M., Vincendon, M., 1980. Structural and conformational investigation of carrageenans. Biopolymers: Original Res. Biomolecules 19 (12), 2165–2175.
Rong, L., Chen, X., Shen, M., Yang, J., Qi, X., Li, Y., Xie, J., 2023. The application of 3D printing technology on starch-based product: A review. Trends. Food Sci. Technol. 134, 149–161.
Savary, G., Handschin, S., Conde-Petit, B., Cayot, N., Doublier, J.-L., 2008. Structure of polysaccharide-starch composite gels by rheology and confocal laser scanning microscopy: effect of the composition and of the preparation procedure. Food Hydrocoll. 22 (4), 520–530.
Severini, C., Derossi, A., Ricci, I., Caporizzi, R., Fiore, A., 2018. Printing a blend of fruit and vegetables. New advances on critical variables and shelf life of 3D edible objects. J. Food Eng. 220, 89–100. https://doi.org/10.1016/j.jfoodeng.2017.08.025.
Sharma, M., Kristo, E., Corredig, M., Duizer, L., 2017. Effect of hydrocolloid type on texture of pureed carrots: rheological and sensory measures. Food Hydrocoll. 63, 478–487.
Shaw, M.T., 2012. Introduction to Polymer Rheology. John Wiley & Sons.
Steele, C.M., Alsanei, W.A., Ayanikalath, S., Barbon, C.E., Chen, J., Cichero, J.A., Coutts, K., Dantas, R.O., Duivestein, J., Giosa, L., 2015. The influence of food texture and liquid consistency modification on swallowing physiology and function: a systematic review. Dysphagia 30, 2–26.
Steffe, J.F., 1996. Rheological methods in food process engineering. Freeman Press.
Stokes, J.R., Boehm, M.W., Baier, S.K., 2013. Oral processing, texture and mouthfeel: from rheology to tribology and beyond. Curr. Opin. Colloid. Interface Sci. 18 (4), 349–359.
Tsai, C., Lin, Y., 2022. Artificial steak: A 3D printable hydrogel composed of egg albumen, pea protein, gellan gum, sodium alginate and rice mill by-products. Future Foods. 5. https://doi.org/10.1016/j.fufo.2022.100121.
Tye, R.J., 1988. The rheology of starch/carrageenan systems. Food Hydrocoll. 2 (4), 259–266.
van Vliet, T., 2002. On the relation between texture perception and fundamental mechanical parameters for liquids and time dependent solids. Food Qual. Prefer. 13 (4), 227–236.
Waterschoot, J., Gomand, S.V., Fierens, E., Delcour, J.A., 2015. Production, structure, physicochemical and functional properties of maize, cassava, wheat, potato and rice starches. Starch-Stärke 67 (1-2), 14–29.
Weenen, H., Van Gemert, L., Van Doorn, J., Dijksterhuis, G., De Wijk, R., 2003. Texture and mouthfeel of semisolid foods: commercial mayonnaises, dressings, custard desserts and warm sauces. J. Texture Stud. 34 (2), 159–179.
Willett, J., Millard, M., Jasberg, B., 1997. Extrusion of waxy maize starch: melt rheology and molecular weight degradation of amylopectin. Polymer. (Guildf) 38 (24), 5983–5989.
Winnik, M.A., Yekta, A., 1997. Associative polymers in aqueous solution. Curr. Opin. Colloid. Interface Sci. 2 (4), 424–436.
Xie, F., Yu, L., Su, B., Liu, P., Wang, J., Liu, H., Chen, L., 2009. Rheological properties of starches with different amylose/amylopectin ratios. J. Cereal. Sci. 49 (3), 371–377.
Yang, F., Cui, Y., Guo, Y., Yang, W., Liu, X., Liu, X., 2021. Internal structure and textural properties of a milk protein composite gel construct produced by three-dimensional printing. J. Food Sci. 86 (5), 1917–1927.
Yang, F., Zhang, M., Bhandari, B., Liu, Y., 2018. Investigation on lemon juice gel as food material for 3D printing and optimization of printing parameters. Lwt 87, 67–76.
Yu, L., Christie, G., 2005. Microstructure and mechanical properties of orientated thermoplastic starches. J. Mater. Sci. 40, 111–116.
Zhang, S., Fu, Q., Li, H., Li, Y., Wu, P., Ai, S., 2024. Polydopamine-coated lignin nanoparticles in polysaccharide-based films: A plasticizer, mechanical property enhancer, anti-ultraviolet agent and bioactive agent. Food Hydrocoll. 147, 109325.
Zhang, S., Fu, Q., Li, H., Wu, P., Waterhouse, G.I., Li, Y., Ai, S., 2023. A pectocellulosic bioplastic from fruit processing waste: robust, biodegradable, and recyclable. Chem. Eng. J. 463, 142452.